

# UCSF

## UC San Francisco Previously Published Works

### Title

Control of cytoplasmic and nuclear protein kinase A by phosphodiesterases and phosphatases in cardiac myocytes

### Permalink

<https://escholarship.org/uc/item/6pj8b1pd>

### Journal

Cardiovascular Research, 102(1)

### ISSN

1015-5007

### Authors

Slimane, Zeineb Haj  
Bedioune, Ibrahim  
Lechêne, Patrick  
et al.

### Publication Date

2014-04-01

### DOI

10.1093/cvr/cvu029

Peer reviewed

# Control of cytoplasmic and nuclear protein kinase A by phosphodiesterases and phosphatases in cardiac myocytes

Zeineb Haj Slimane<sup>1,2</sup>, Ibrahim Bedioune<sup>1,2</sup>, Patrick Lechêne<sup>1,2</sup>, Audrey Varin<sup>1,2</sup>, Florence Lefebvre<sup>1,2</sup>, Philippe Mateo<sup>1,2</sup>, Valérie Domergue-Dupont<sup>2</sup>, Matthias Dewenter<sup>3</sup>, Wito Richter<sup>4</sup>, Marco Conti<sup>4</sup>, Ali El-Armouche<sup>3,5</sup>, Jin Zhang<sup>6</sup>, Rodolphe Fischmeister<sup>1,2</sup>, and Grégoire Vandecasteele<sup>1,2\*</sup>

<sup>1</sup>INSERM UMR-S 769, Châtenay-Malabry, France; <sup>2</sup>Faculty of Pharmacy, University Paris-Sud LabEx LERMIT, DHU TORINO, IFR141, Châtenay-Malabry, France; <sup>3</sup>Department of Pharmacology, University Medical Center Göttingen (UMG) Heart Center, Georg August University Medical School, Göttingen, Germany; <sup>4</sup>Department of Obstetrics, Gynecology, and Reproductive Sciences, Center for Reproductive Sciences, University of California, San Francisco, CA, USA; <sup>5</sup>Department of Pharmacology, University of Technology, Dresden, Germany; and <sup>6</sup>Department of Pharmacology and Molecular Sciences, Johns Hopkins University School of Medicine, Baltimore, MD, USA

Received 22 September 2013; revised 20 December 2013; accepted 24 January 2014; online publish-ahead-of-print 18 February 2014

Time for primary review: 45 days

## Aims

The cAMP-dependent protein kinase (PKA) mediates  $\beta$ -adrenoceptor ( $\beta$ -AR) regulation of cardiac contraction and gene expression. Whereas PKA activity is well characterized in various subcellular compartments of adult cardiomyocytes, its regulation in the nucleus remains largely unknown. The aim of the present study was to compare the modalities of PKA regulation in the cytoplasm and nucleus of cardiomyocytes.

## Methods and results

Cytoplasmic and nuclear cAMP and PKA activity were measured with targeted fluorescence resonance energy transfer probes in adult rat ventricular myocytes.  $\beta$ -AR stimulation with isoprenaline (Iso) led to fast cAMP elevation in both compartments, whereas PKA activity was fast in the cytoplasm but markedly slower in the nucleus. Iso was also more potent and efficient in activating cytoplasmic than nuclear PKA. Similar slow kinetics of nuclear PKA activation was observed upon adenylyl cyclase activation with L-858051 or phosphodiesterase (PDE) inhibition with 3-isobutyl-1-methylxanthine. Consistently, pulse stimulation with Iso (15 s) maximally induced PKA and myosin-binding protein C phosphorylation in the cytoplasm, but marginally activated PKA and cAMP response element-binding protein phosphorylation in the nucleus. Inhibition of PDE4 or ablation of the *Pde4d* gene in mice prolonged cytoplasmic PKA activation and enhanced nuclear PKA responses. In the cytoplasm, phosphatase 1 (PP1) and 2A (PP2A) contributed to the termination of PKA responses, whereas only PP1 played a role in the nucleus.

## Conclusion

Our study reveals a differential integration of cytoplasmic and nuclear PKA responses to  $\beta$ -AR stimulation in cardiac myocytes. This may have important implications in the physiological and pathological hypertrophic response to  $\beta$ -AR stimulation.

## Keywords

cAMP-dependent protein kinase • Compartmentation • 3'-5'-cyclic nucleotide phosphodiesterases • Ser/Thr protein phosphatases • Nucleus

## 1. Introduction

The cAMP-dependent protein kinase (PKA) is critically involved in the regulation of cardiac function by catecholamines acting on  $\beta$ -adrenoceptors ( $\beta$ -ARs) as well as several other hormonal and circulating factors acting through other  $G_s$  protein-coupled receptors

( $G_s$ PCRs). In the absence of cAMP, the PKA holoenzyme is a heterotrimer consisting of two catalytic (C) subunits that are bound and inhibited by a dimer of regulatory (R) subunits.  $G_s$ PCR occupancy leads to activation of adenylyl cyclases (ACs) and increases in intracellular [cAMP]. Cooperative binding of cAMP to the R subunits leads to dissociation and activation of the C subunits, which phosphorylate multiple

\* Corresponding author. Tel: +33 1 46 83 57 17; fax: +33 1 46 83 54 75, Email: gregoire.vandecasteele@u-psud.fr

protein targets in various subcellular compartments.<sup>1</sup> In cardiac myocytes, the best described PKA targets are proteins involved in excitation–contraction coupling (ECC) including the sarcolemmal L-type  $\text{Ca}^{2+}$  channel, the ryanodine receptor (RyR2), and phospholamban (PLB), as well as the myofilament proteins such as cardiac myosin-binding protein C (cMyBP-C) and troponin I.<sup>2</sup>

The velocity and specificity of  $\beta$ -AR regulation is determined by the localization of the PKA holoenzyme to its targets by A-kinase anchoring proteins (AKAPs)<sup>3</sup> and by the spatiotemporal pattern of cAMP signalling, which results from the interplay between cAMP production by ACs and cAMP degradation by cyclic nucleotide phosphodiesterases (PDEs).<sup>4</sup> In addition, PKA activity is counterbalanced by Ser/Thr protein phosphatases (PPs).<sup>5</sup> In cardiac myocytes, the PDEs that degrade cAMP belong to five major families (PDE1–4 and PDE8),<sup>4</sup> whereas the major cardiac PPs are PP1, PP2A, and PP2B.<sup>5</sup>

The development of genetically encoded indicators of cAMP levels and PKA activity has been instrumental in defining the spatiotemporal characteristics of cAMP signals and PKA activity elicited by  $G_s$ PCRs in living cardiac myocytes. The use of targeted sensors to various intracellular compartments revealed subcellular compartments with distinct cAMP responses and PKA phosphorylation gradients upon  $\beta$ -AR stimulation.<sup>6,7</sup> These studies also identified the cAMP-specific PDE4 family as a major negative regulator of cAMP generated by  $\beta$ -ARs.<sup>6</sup> Three genes encoding PDE4 (*Pde4a*, *Pde4b*, and *Pde4d*) are expressed in cardiac tissue, and recent studies have emphasized the importance of PDE4B and PDE4D for  $\beta$ -AR regulation of cardiac ECC (reviewed in<sup>4</sup>).

PKA regulates numerous other effectors in cardiac myocytes, notably the transcription factors belonging to the cAMP response element-binding protein (CREB) family and Class II histone deacetylase (HDAC) 4 and 5 in the nucleus.<sup>8–11</sup> According to the classical view of nuclear PKA signalling, cAMP binds to PKA outside of the nucleus and, after dissociation from the R subunits, the C subunits cross the nuclear envelope by passive diffusion, which is a slow process.<sup>12</sup> However, recent evidence indicates that, in HEK293 cells, a nuclear resident pool of PKA exists, but is isolated from cAMP generated at the plasma membrane by AKAP-anchored PDE4.<sup>13</sup> In cardiac myocytes, it was reported that muscle AKAP (mAKAP) targets PKA to multiple subcellular compartments, including the nucleus<sup>14</sup> and the nuclear membrane.<sup>15</sup> Moreover, mAKAP binds PDE4D3, a specific PDE4 isoform, which may control cAMP levels in this compartment and thereby the release of PKA C subunits into the nucleus.<sup>16,17</sup> However, the modalities of nuclear PKA regulation in adult cardiomyocytes remain unknown. This issue is important, given the role of the mAKAP complex and Class II HDACs in the control of pathological cardiac hypertrophy<sup>17,18</sup> and of the CREB family of transcription factors in multiple aspects of cardiac function, including hypertrophy and apoptosis<sup>19</sup> as well as the deleterious effects of chronic  $\beta_1$ -AR overexpression in the heart.<sup>20</sup>

In this study, we compared the spatiotemporal dynamics of cytoplasmic and nuclear cAMP and PKA activity in adult cardiac myocytes using recombinant fluorescence resonance energy transfer (FRET) probes targeted to these compartments. We found that, upon  $\beta$ -AR stimulation, cAMP increases with similar fast kinetics in both compartments, whereas PKA activation is considerably delayed in the nuclei compared with the cytoplasm. Our results reveal for the first time the respective roles of PDE3 and PDE4 and of PP1, PP2A, and PP2B in the differential integration of cytoplasmic and nuclear PKA responses to  $\beta$ -AR stimulation in cardiac myocytes.

## 2. Methods

All experiments performed conform to the European Community guiding principles in the care and use of animals (86/609/CEE, CE Off J no. L358, 18 December 1986), the local ethics committee (CREEA Ile-de-France Sud) guidelines, and the French decree no. 87-848 of 19 October 1987 (J Off République Française, 20 October 1987, pp. 12 245–12 248). Authorizations to perform animal experiments according to this decree were obtained from the French Ministère de l'Agriculture, de la Pêche et de l'Alimentation (no. D 92-283, 13 December 2012). A total of 72 rats and 7 mice were used for this study.

### 2.1 FRET-based sensors of cAMP and PKA activity

Cytoplasmic cAMP was measured using the indicator of cAMP using Epac 3 (ICUE3), a FRET-based sensor.<sup>21</sup> Nuclear localization of ICUE3 was achieved by adding a C-terminal nuclear localization signal (ICUE3-NLS).<sup>13</sup> PKA activity was measured with the FRET-based A-kinase activity reporter 3 (AKAR3).<sup>22</sup> Because untargeted AKAR3 is localized both in the cytoplasm and the nucleus, a specific cytoplasmic localization of AKAR3 was achieved by adding a C-terminal nuclear export signal to AKAR3 (AKAR3-NES). A specific nuclear localization was obtained by adding a C-terminal NLS (AKAR3-NLS).<sup>22</sup> Adenoviruses encoding Ad.AKAR3-NES and Ad.AKAR3-NLS were generated using the ViraPower Adenoviral Expression System (Invitrogen) according to the manufacturer's protocol. The adenovirus encoding ICUE3 was kindly provided by Dr Yang K. Xiang (University of California, Davis, CA, USA). The adenovirus encoding ICUE3-NLS was generated by Welgen, Inc.

### 2.2 Isolation of adult rat ventricular myocytes

Male Wistar rats (200–250 g) were subjected to anaesthesia by intraperitoneal injection of pentothal (0.1 mg/g). Individual ventricular myocytes were obtained by retrograde perfusion of the hearts as previously described.<sup>23</sup> See Supplementary material online for details.

### 2.3 Adenoviral infection

The medium was replaced by 300  $\mu\text{L}$  of FBS-free MEM containing one of the following adenoviruses: Ad-AKAR3-NES, Ad-AKAR3-NLS, Ad-ICUE3, or Ad-ICUE3-NLS. In some experiments, PKA was blocked by co-infecting the cells with adenoviruses encoding a rabbit muscle PKA inhibitor (Ad.PKI)<sup>24</sup>. All experiments were done 24–48 h after cell isolation.

### 2.4 FRET measurements of cytoplasmic and nuclear cAMP and PKA activity

Cells were maintained at room temperature (20–25°C) in the same Ringer solution as described above. Images were captured every 5 s using the  $\times 40$  oil immersion objective of an inverted microscope (Nikon) connected to a Cool SNAP HQ2 camera (Photometrics) controlled by the Metafluor software (Molecular Devices). Cyan Fluorescent Protein (CFP) was excited during 300 ms by a Xenon lamp (Nikon) using a 440/20BP filter and a 455LP dichroic mirror. Dual-emission imaging of CFP and Yellow Fluorescent Protein (YFP) was performed using a Dual-View emission splitter equipped with a 510 LP dichroic mirror and BP filters 480/30 and 535/25 nm, respectively.

### 2.5 Western blot studies

Adult rat ventricular myocytes (ARVMs) were lysed in cold HNTG buffer, proteins were resolved by SDS–PAGE and transferred to nitrocellulose membranes. Total and phosphospecific antibodies against CREB and cMyBP-C and a calsequestrin antibody were used as detailed in Supplementary material online.

## 2.6 Data analysis

For FRET measurements with AKAR3-NES and ICUE3, average fluorescence intensity was measured in the entire cell or in a portion of the cytoplasm with identical results. For AKAR3-NLS and ICUE3-NLS, average fluorescence intensity was measured in a region of interest inside the nuclei. Background was subtracted and YFP intensity was corrected for CFP bleed through before calculating the ratio. Ratio images were obtained with the ImageJ software. Average time course of the ratio represents the mean of all cells measured in a given experimental condition. The data were normalized to the ratio measured before the stimulus and expressed as per cent change over basal. Student's *t*-test was used to compare two groups. Western blot data were compared with the Mann–Whitney test. Concentration-response curves (CRCs) were compared by Fisher's test. A *P*-value of <0.05 was considered statistically significant. Densitometric analyses of western blots were performed using the Quantity one software (Bio-Rad).

## 3. Results

### 3.1 Real-time measurements of cytoplasmic and nuclear PKA activities in ARVMs

Adenoviruses were generated to express the FRET-based AKAR3 targeted to the cytoplasm (AKAR3-NES) and the nucleus (AKAR3-NLS)

in ARVMs. YFP emission images were acquired by confocal microscopy to examine their subcellular localization. As shown in *Figure 1A*, myocytes infected at a multiplicity of infection (MOI) of 1000 active viral particles per cell showed AKAR3-NES expression in the cytoplasm but not in the nuclei 24 h after infection. AKAR3-NLS expression could be detected slightly earlier (18 h) in the nuclei and was excluded from the cytoplasm (*Figure 1B*). However, this specific localization was dependent on the time of expression and was completely lost at 48 h, unless the MOI was reduced to 200 (see Supplementary material online, *Figure S1*). In order to test the functionality of AKAR3 in each compartment, cells infected with Ad.AKAR3-NES or Ad.AKAR3-NLS at MOI 1000 for 24 h were stimulated with the  $\beta$ -AR agonist isoprenaline (Iso, 1  $\mu$ M), and the CFP and YFP fluorescence were measured simultaneously in the entire cell for AKAR3-NES and in the two nuclei for AKAR3-NLS (*Figure 1C* and *D*). As shown in the graphs and the corresponding pseudocolor images, Iso strongly increased the YFP/CFP ratio in the cytoplasm and also in both nuclei. The average change was significantly larger in the cytoplasm ( $+38.6 \pm 2.1\%$ ) than in the nuclei ( $+20.4 \pm 2.1\%$ ,  $P < 0.001$ ), and both were abolished by application of the PKA inhibitor H89 (10  $\mu$ M) or by co-expression of the PKA inhibitor peptide PKI (*Figure 1E* and *F*). In the absence of Iso, neither H89 nor PKI had any effect on the basal YFP/CFP ratio in the cytoplasm or in the nuclei (see Supplementary material online, *Figure S2*). To further characterize

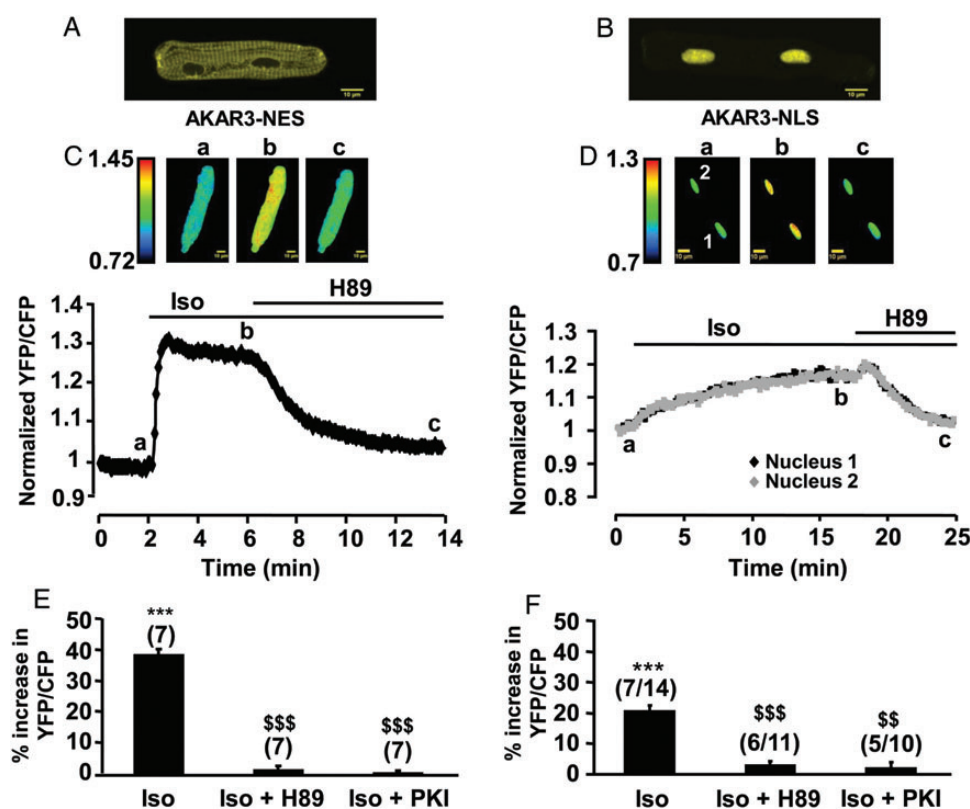


**Figure 1** Measurements of cytoplasmic and nuclear PKA activities in ARVMs. (A and B) Confocal Yellow Fluorescent Protein (YFP) images of ARVMs infected with Ad.AKAR3-NES (A) and Ad.AKAR3-NLS (B). Scale bars: 10  $\mu$ m. (C and D) Time course of the normalized YFP/Cyan Fluorescent Protein (CFP) ratio upon  $\beta$ -AR stimulation by Iso (1  $\mu$ M) alone and after addition of the PKA inhibitor H89 (10  $\mu$ M) in myocytes expressing AKAR3-NES (C) or AKAR3-NLS (D). Pseudo-colour images of the YFP/CFP ratio were recorded at the times indicated by the letters on the graphs. (E and F) Mean variation ( $\pm$  SEM) of the YFP/CFP ratio upon stimulation with Iso (1  $\mu$ M) in the presence or absence of H89 or PKI in ARVMs expressing AKAR3-NES (E) or AKAR3-NLS (F). PKI was overexpressed by adenoviral infection. In (E), the numbers above the bars indicate the number of cells. In (F), the first number above the bars indicates the number of cells and the second indicates the number of nuclei. Data are from eight rats. Statistical significance is indicated as \*\*\* $P < 0.001$  vs. control; \$\$\$ $P < 0.01$  vs. Iso; \$\$\$ $P < 0.001$  vs. Iso.

PKA activation by  $\beta$ -AR stimulation in the two compartments, CRCs to Iso were generated. Supplementary material online, *Figure S3A* shows a typical experiment in a myocyte expressing AKAR3-NES and exposed to increasing concentrations of Iso between 0.1 nM and 1  $\mu$ M. The YFP/CFP emission ratio increased in a concentration-dependent manner until 30 nM Iso, and the effect was fully reversible upon washout. Supplementary material online, *Figure S3B* compares the average CRC obtained in the cytoplasm (black squares) and in the nucleus (white squares). Hill fit of the data yielded apparent maximal effects ( $E_{max}$ ) of  $+46.1 \pm 2.1$  and  $+27.6 \pm 6.2\%$ , and half-maximal activation values ( $EC_{50}$ ) of  $1.8 \pm 0.3$  and  $4.2 \pm 1.0$  nM in the cytoplasm and the nuclei, respectively. The two curves were statistically different as indicated by Fisher's test ( $P < 0.001$ ). When CRCs to Iso were repeated in ARVMs infected with Ad.AKAR3-NES or Ad.AKAR3-NLS at MOI 1000 during 48 h and the fluorescence was measured in the entire cell, these differences were no longer observed (see Supplementary material online, *Figure S4*). Thus, the decreased efficiency and potency of Iso in the nucleus compared with the cytoplasm cannot be attributed to different properties of the targeted probes.

### 3.2 Kinetics of cAMP and PKA activation in the cytoplasm and in the nucleus of cardiac myocytes

In addition to these steady-state differences, the kinetics of PKA activation was much faster in the cytoplasm than in the nuclei upon  $\beta$ -AR stimulation (*Figure 2A* and *B*). Indeed, half-maximal PKA activation ( $t_{1/2\ on}$ ) was reached  $\sim 30$  s after addition of Iso in the cytoplasm, but required  $\sim 3$  min in the nuclei (*Figure 2B*). This difference was also observed upon direct AC activation with the hydrosoluble forskolin analogue L-858051 (L-85, 30  $\mu$ M, *Figure 2C* and *D*) or upon global PDE blockade with 3-isobutyl-1-methylxantine (IBMX) (300  $\mu$ M, *Figure 2E* and *F*). In both compartments, the response to Iso was faster than that to L-85 and to IBMX, and in the case of L-85, the maximal nuclear PKA activation ( $+38.8 \pm 1.5\%$ ) was significantly higher than that obtained with Iso ( $+21.4 \pm 2.4\%$ ,  $P < 0.001$  vs. L-85) or IBMX ( $+22.1 \pm 3.1\%$ ,  $P < 0.01$  vs. L-85). To test whether restricted cAMP diffusion could be involved in the slow phosphorylation of AKAR3-NLS upon  $\beta$ -AR stimulation, we compared the kinetics of cAMP in the cytoplasm and the nuclei using the untargeted cAMP sensor, ICUE3<sup>21</sup> and a nuclear version of the

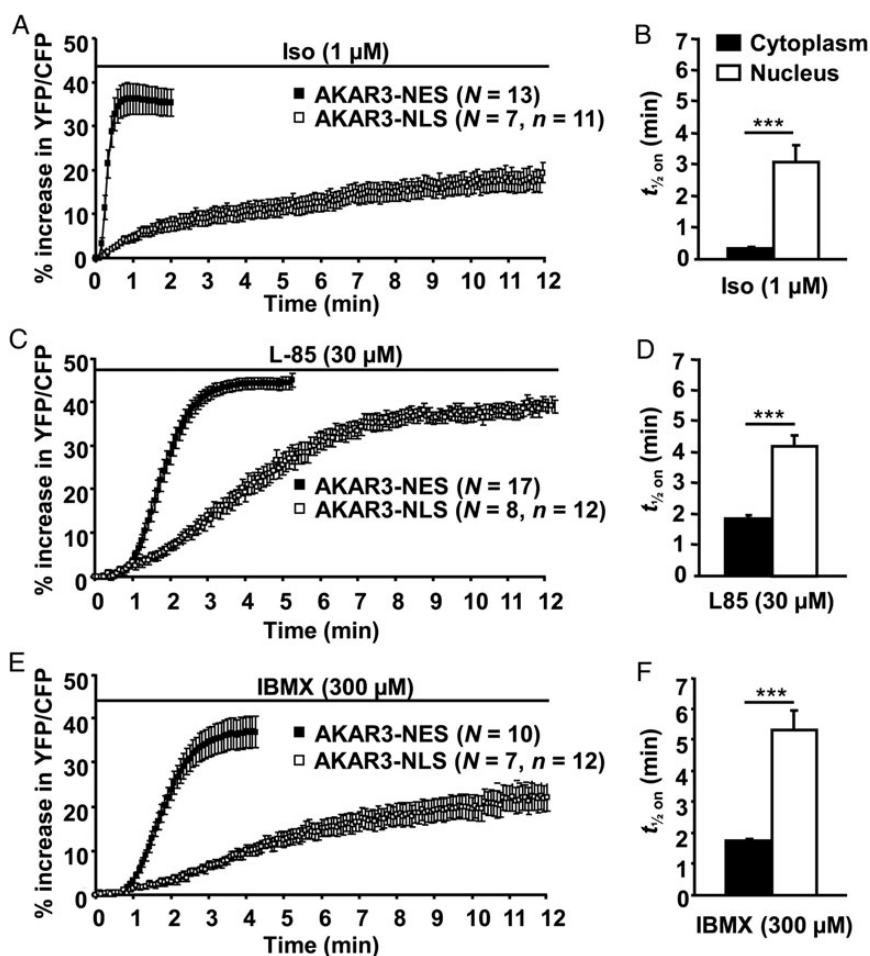


**Figure 2** Comparative kinetics of cytoplasmic and nuclear PKA activation in response to different cAMP-elevating agents in ARVMs. Average time courses of the normalized YFP/CFP ratio obtained from myocytes expressing AKAR3-NES (black squares) and AKAR3-NLS (white squares) upon (A),  $\beta$ -AR stimulation with Iso (1  $\mu$ M), (C) direct AC activation with L-858051 (L-85, 30  $\mu$ M), and (E) global PDE inhibition with 3-isobutyl-1-methylxantine (300  $\mu$ M).  $N$  refers to the number of cells, and  $n$  refers to the number of nuclei. Each symbol on the graphs represents the mean ( $\pm$  SEM). (B, D, and F) PKA activation kinetics ( $t_{1/2\ on}$ ) obtained from experiments shown in (A, C, and E), respectively. Data are from 10 rats. Statistical significance is indicated as \*\*\* $P < 0.001$ .



sensor, ICUE3-NLS.<sup>13</sup> Myocytes infected with Ad.ICUE3 and Ad.ICUE3-NLS expressed the probe in the cytoplasm and nuclei, respectively (Figure 3A).  $\beta$ -AR stimulation with Iso (1  $\mu$ M) produced a fast increase in cAMP with similar onset kinetics ( $t_{1/2\text{ on}} \sim 20$  s) in both compartments (Figure 3B and C).

In a next series of experiments, we compared the effect of a transient  $\beta$ -AR stimulation (Iso, 100 nM, 15 s) similar to those elicited by a startle response on cytoplasmic and nuclear PKA activities. As shown in Figure 4A, this induced a maximal activation of PKA in the cytoplasm ( $+49.7 \pm 2.0\%$ ,  $P < 0.001$ ), but a marginal increase in the nuclei ( $+3.2 \pm 0.9\%$ ,  $P < 0.01$ ). Similar differences were observed when comparing the PKA phosphorylation of myofilament protein cMyBP-C at Ser282 with that of the nuclear transcription factor CREB at Ser133. cMyBP-C was significantly phosphorylated upon a short (15 s) Iso stimulation (Figure 4C), while CREB was not (Figure 4D). Prolonging the Iso application to 15 min did not further increase cMyBP-C phosphorylation (Figure 4C), but significantly increased CREB phosphorylation (Figure 4D). In parallel experiments, we verified that Iso stimulation

(100 nM, 15 s and 15 min) did not modify total cMyBP-C and CREB protein levels (see Supplementary material online, Figure S5). These results suggest that the PKA-dependent regulation of contractility can be dissociated from regulation of gene expression during short  $\beta$ -AR stimulation.

### 3.3 Regulation of cytoplasmic and nuclear PKA activities in cardiac myocytes

We next sought to characterize the regulatory mechanisms governing PKA activation in the two compartments. We have shown previously that PDE3 and PDE4 account for the majority of the cAMP-hydrolyzing activity in ARVMs, and that PDE4 is predominant in the degradation of cAMP generated by  $\beta$ -ARs at the plasma membrane and in the cytoplasm.<sup>6</sup> Therefore, we examined the respective contribution of these PDEs to the regulation of PKA activity in the cytoplasm and in the nuclei using the specific PDE3 inhibitor cilostamide (Cil) and the specific PDE4 inhibitor Ro 20-1724 (Ro). Neither Cil (1  $\mu$ M) alone nor Ro (10  $\mu$ M) alone had any effect on the basal YFP/CFP ratio (see Supplementary material online, Figure S6). ARVMs overexpressing AKAR3-NES and AKAR3-NLS were briefly exposed to Iso (100 nM, 15 s) in the presence of Cil or Ro. Each inhibitor was applied during 3 min before the Iso pulse and continuously thereafter. As illustrated in Figure 5, PDE3 inhibition with Cil did not alter cytoplasmic or nuclear PKA activation by Iso (Figure 5A and B), whereas Ro greatly prolonged PKA activation in the cytoplasm ( $t_{1/2\text{ off}} = 3.4 \pm 0.2$  vs.  $1.7 \pm 0.1$  min for Iso alone,  $P < 0.001$ ) and in the nuclei (Figure 5C and D). Because in cardiac myocytes PDE4D is enriched at the nuclear envelope,<sup>16,17,25</sup> we examined  $\beta$ -AR regulation of cytoplasmic and nuclear PKA activities in adult mouse ventricular myocytes (AMVMs) from *Pde4d*-deficient (*Pde4d*<sup>-/-</sup>) mice.<sup>26</sup> In these myocytes, the response to Iso pulse stimulation in the cytoplasm was slightly, but significantly prolonged compared with WT myocytes ( $t_{1/2\text{ off}} = 2.4 \pm 0.3$  min in *Pde4d*<sup>-/-</sup> vs.  $1.5 \pm 0.2$  min, in WT,  $P < 0.05$ , Figure 5E). In the nuclei, similar to what we observed in ARVMs, Iso pulse stimulation had virtually no effect on PKA activity in WT AMVMs ( $+1.0 \pm 0.5\%$ ,  $P < 0.01$ , Figure 5F). However, in *Pde4d*<sup>-/-</sup> myocytes, Iso stimulation increased nuclear PKA activity approximately four-fold ( $+3.8 \pm 0.9\%$  in *Pde4d*<sup>-/-</sup> vs. WT,  $P < 0.05$ , Figure 5F). These results are consistent with PDE4D being an important regulator of nuclear cAMP/PKA signalling.

### 3.4 Contribution of Ser/Thr PPs to the regulation of cytoplasmic and nuclear PKA responses in ARVMs

In cardiac myocytes, PP1 and PP2A are the major Ser/Thr PPs that counterbalance PKA activity. To assess the contribution of these PPs to the modulation of the cytoplasmic and nuclear PKA responses, FRET experiments were performed in ARVMs expressing AKAR3-NES or AKAR3-NLS exposed to Iso pulse (100 nM, 15 s) in the presence of Calyculin A (CalyA, 100 nM), which inhibits both PP1 and PP2A. As shown in Figure 6A, CalyA markedly slowed down the dephosphorylation of AKAR3 by Iso in the cytoplasm ( $t_{1/2\text{ off}} = 7.0 \pm 1.6$  vs.  $1.5 \pm 0.1$  min for Iso alone,  $P < 0.05$ ), and unmasked a strong PKA response in the nucleus, which remained sustained for at least 8 min (Figure 6B). To determine the participation of PP2A to these effects, okadaic acid (OA) was used at a concentration of 100 nM, at which it preferentially inhibits this PP.<sup>27</sup> As shown in Figure 6C, OA also slowed down the dephosphorylation of AKAR3 in the cytoplasm ( $t_{1/2\text{ off}} = 3.0 \pm 0.3$  vs.  $1.5 \pm 0.1$  min for Iso alone,  $P < 0.001$ ), although to a lesser extent

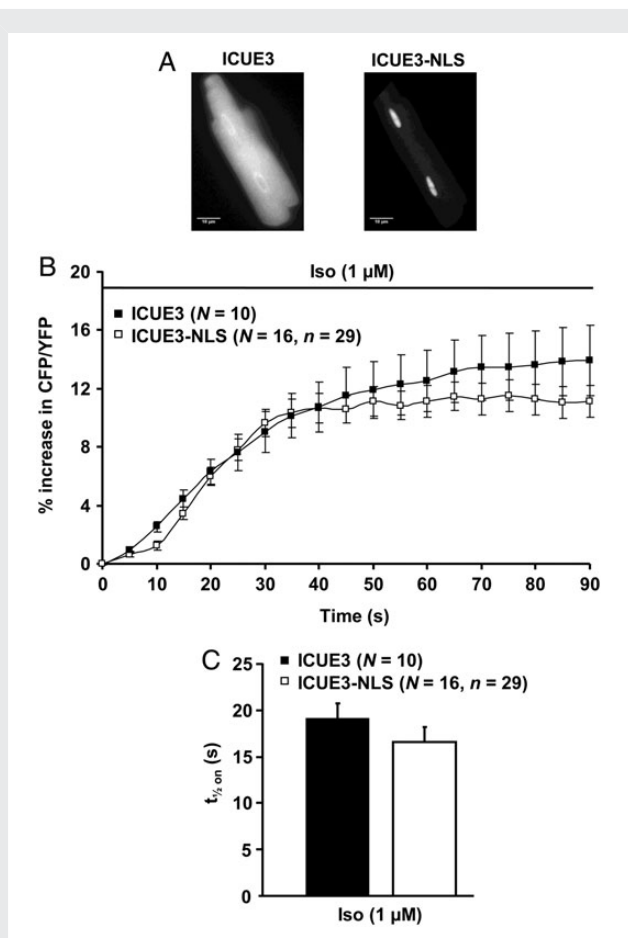


**Figure 3** Comparative measurements of cytoplasmic and nuclear cAMP responses to a maintained  $\beta$ -AR stimulation in ARVMs. (A) YFP images of ARVMs infected with Ad.ICUE3 or Ad.ICUE3-NLS at MOI 1000 during 24 and 16 h, respectively. (B) Average time courses of the normalized CFP/YFP ratio during upon  $\beta$ -AR stimulation with Iso (1  $\mu$ M) in myocytes expressing ICUE3 (black squares) or ICUE3-NLS (white squares). Each symbol represents the mean ( $\pm$  SEM). (C) Kinetics of cAMP elevation ( $t_{1/2\text{ on}}$ ) obtained from experiments shown in (B). Bar graphs represent the mean  $\pm$  SEM. Data are from five rats.

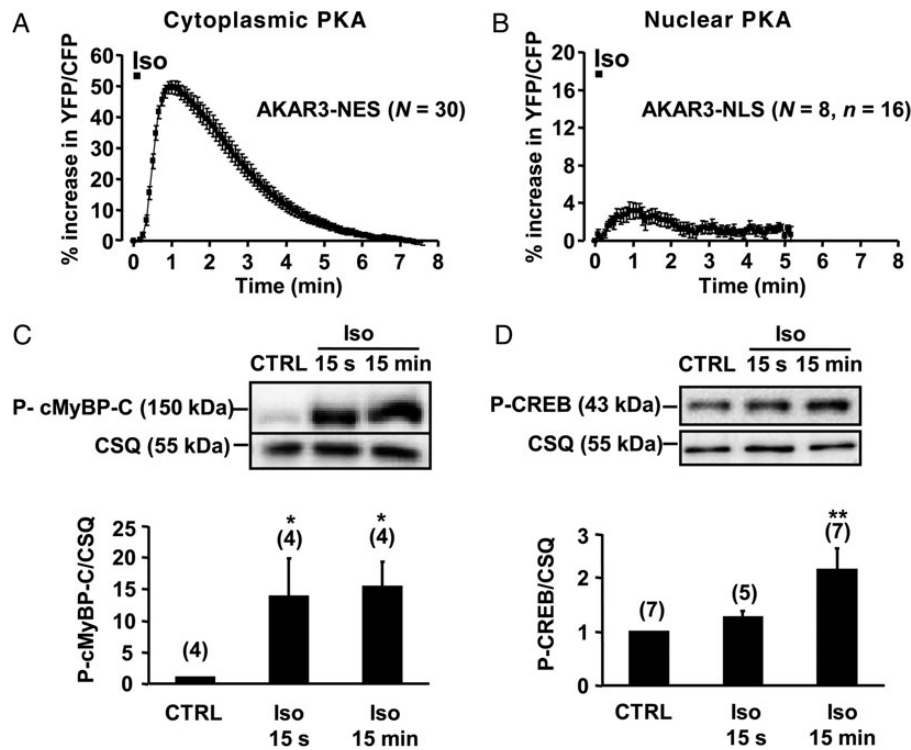


**Figure 4** Comparison of cytoplasmic and nuclear PKA responses upon brief  $\beta$ -AR stimulation in ARVMs. (A and B) Average time course of cytoplasmic and nuclear PKA activities induced by Iso (100 nM, 15 s) in ARVMs expressing AKAR3-NES (A) and AKAR3-NLS (B). Each symbol represents the mean ( $\pm$  SEM). (C and D) Phosphorylation levels of cMyBP-C (C) and CREB (D) in ARVMs treated or not with 100 nM Iso for 15 s or 15 min. Calsequestrin (CSQ) was used as a loading control. Bar graphs represent the mean  $\pm$  SEM, and the numbers above the bars indicate the number of independent experiments. Data are from 19 rats. Statistical significance between control and Iso conditions is indicated as: \* $P < 0.05$ ; \*\* $P < 0.01$ .

than CalyA ( $P < 0.001$ ). In contrast, OA had no effect on the nuclear PKA response to Iso pulse stimulation (Figure 6D). In another series of experiments, a potential role for PP2B (calcineurin) was investigated using the PP2B-selective inhibitor cyclosporin A (CsA, 5  $\mu$ M). As shown in Figure 6E and F, CsA did not modify the PKA response to Iso, neither in the cytoplasm nor in the nucleus. Taken together, these results indicate that, upon  $\beta$ -AR stimulation, PP1 and PP2A contribute to the AKAR3 dephosphorylation in the cytoplasm, whereas PP1 plays a major role in the nucleus.

## 4. Discussion

Although it is known that PKA can regulate cardiac gene expression through nuclear transcription factors such as CREB and specific Class II HDACs, the modalities of nuclear PKA regulation have remained elusive in cardiac myocytes. Here, we show the dynamics of this regulation in response to  $\beta$ -AR stimulation in living adult cardiomyocytes. Our results indicate that  $\beta$ -AR stimulation of nuclear PKA activity is temporally dissociated from that of nuclear cAMP elevation and from that of cytoplasmic PKA activation. This is consistent with activation of the PKA holoenzyme in the cytoplasm and translocation of the C subunits to the nucleus. We show that PDE4 is an upstream negative regulator of this process, with PDE4D playing an important role in controlling nuclear PKA activity, whereas PP1 and PP2A are downstream negative regulators. Importantly, the contribution of PP1 and PP2A to the termination of the  $\beta$ -AR PKA response differs between these two compartments, with PP1 being predominant in the nucleus.

One major finding was that, independently of the mechanism of cAMP elevation, the kinetics of PKA activation was much slower in the nuclei than in the cytoplasm, as previously reported in model cell lines<sup>13,22</sup> and primary neurons.<sup>28</sup> Importantly, when measuring cytoplasmic and nuclear cAMP upon  $\beta$ -AR stimulation, no such delay was observed (Figure 3) indicating that limited cAMP diffusion was not the cause of the slow increase in nuclear PKA activity. This was consistent with activation of PKA holoenzyme in the cytoplasm and slow translocation of the C subunits into the nuclei by passive diffusion.<sup>12</sup> As a result, a short  $\beta$ -AR stimulation marginally activated PKA and CREB phosphorylation in the nuclei, while it maximally activated PKA and cMyBP-C phosphorylation in the cytoplasm (Figure 4). Such temporal dissociation of PKA action in the two compartments may have important implications for cardiac physiology and pathology. The fast kinetics of cytoplasmic PKA activation observed here closely mimic the kinetics of L-type  $\text{Ca}^{2+}$  current stimulation<sup>6</sup> and emphasize the importance of fast PKA activation for the velocity and efficiency of the fight-or-flight response. The modest consequences on nuclear PKA activity and CREB phosphorylation suggest that PKA regulation of cardiac contractility can be dissociated from regulation of gene expression during short-term sympathetic stimulation. However, cAMP may also activate other effectors such as Epac, which was shown to be localized not only at the plasma membrane but also at the nuclear/perinuclear area in cardiomyocytes.<sup>17,29</sup> In adult rat ventricular myocytes, Epac activation was shown to contribute to the pro-hypertrophic effects of  $\beta$ -AR stimulation<sup>30</sup> in part by increasing nuclear  $[\text{Ca}^{2+}]$  and CaMKII-dependent nuclear export of HDAC5, with consequent derepression of the

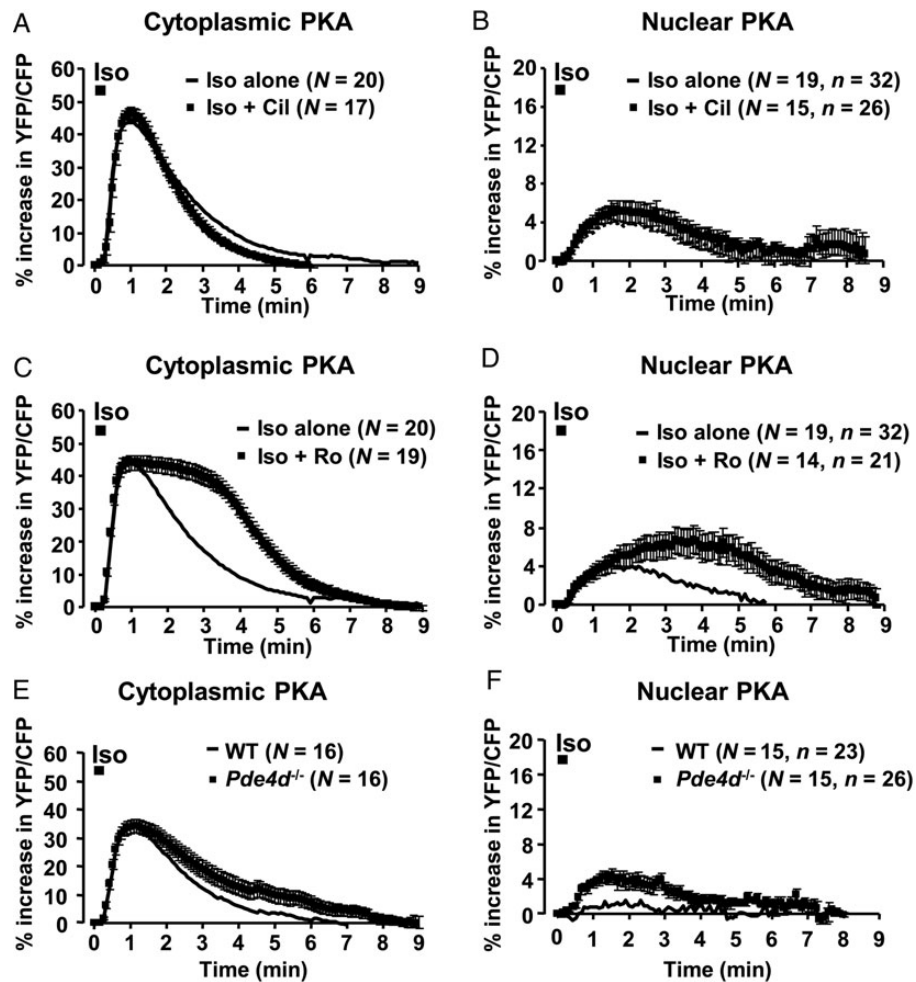


**Figure 5** Role of PDE3 and PDE4 in the regulation of cytoplasmic and nuclear PKA activities. (A and B) Effect of PDE3 inhibition with 1  $\mu$ M Cil (black squares) on cytoplasmic (A) and nuclear (B) PKA responses to Iso (100 nM, 15 s) in ARVMs expressing AKAR3-NES and AKAR3-NLS, respectively. (C and D) Effect of PDE4 inhibition with 10  $\mu$ M Ro (black squares) on cytoplasmic (C) and nuclear (D) PKA responses to Iso (100 nM, 15 s) in ARVMs expressing AKAR3-NES and AKAR3-NLS, respectively. Cil or Ro was applied 3 min before a 15 s pulse of Iso and then maintained throughout the experiments. Solid lines indicate the effect of Iso alone. Data are from four rats. (E and F) Effect of *Pde4d* gene ablation on Iso (100 nM, 15 s)-induced activation of PKA in the cytoplasm (E) and the nuclei (F) in AMVMs from wild-type (WT, solid lines) and PDE4D-deficient (*Pde4d*<sup>-/-</sup>, black squares) AMVMs. Data are from seven mice. Each symbol in A–F represents the mean  $\pm$  SEM.

transcription factor MEF2.<sup>29</sup> Our results also show that sustained  $\beta$ -AR activation, as may occur during intense and prolonged physical exercise or following myocardium injury, increases nuclear PKA activity and CREB phosphorylation. While the CREB/CREM family of transcription factors may contribute to  $\beta$ -AR-dependent maladaptive remodelling,<sup>19,20</sup> PKA can also phosphorylate HDAC5 in the nucleus.<sup>9,11</sup> This, in contrast to phosphorylation by CaMKII and PKD,<sup>31–33</sup> favours its nuclear retention, and the repression of the hypertrophic gene programme.<sup>9,11</sup> Altogether these results illustrate the dynamic and versatile nature of nuclear cAMP signalling, which may exert both beneficial and detrimental influences on the adult heart depending on the respective balance between the different target effectors.

Our finding that PDE4 inhibition strongly prolonged  $\beta$ -AR stimulation of PKA activity in the cytoplasm, whereas PDE3 had no effect, is consistent with the relative contribution of these two PDE families to cAMP degradation in the cytoplasm of ARVMs following a short  $\beta$ -AR

stimulation.<sup>6</sup> Analysis of cardiomyocytes from *Pde4d*<sup>-/-</sup> mice further shows the participation of this specific isoform to termination of  $\beta$ -AR responses in ARVMs, which is consistent with the reported role of PDE4D in potentiating  $\beta$ -AR-stimulated contraction rate in neonatal cardiomyocytes from *Pde4d*<sup>-/-</sup><sup>34</sup> and the reported roles of PDE4D variants in  $\beta$ -AR signalling and ECC in heart.<sup>4,35,36</sup> PDE3 and PDE4 represent the major PDE activities in cardiac nuclei and are primarily localized at the nuclear envelope.<sup>25</sup> Here, we show that, following short  $\beta$ -AR stimulation, PDE4 predominates to control nuclear PKA activation. Results in cardiomyocytes from *Pde4d*<sup>-/-</sup> mice further indicate that the lack of PDE4D enhanced nuclear PKA responses to  $\beta$ -AR stimulation, which is consistent with the presence this isoform at the nuclear membrane.<sup>16,17,25</sup> Because at the nuclear envelope, PDE4D is integrated in a macromolecular complex including mAKAP and is involved in the regulation of cardiomyocyte hypertrophy,<sup>17,37</sup> our results suggest that dysregulation of nuclear PKA activity following the loss of PDE4D may participate in the late onset dilated cardiomyopathy observed in



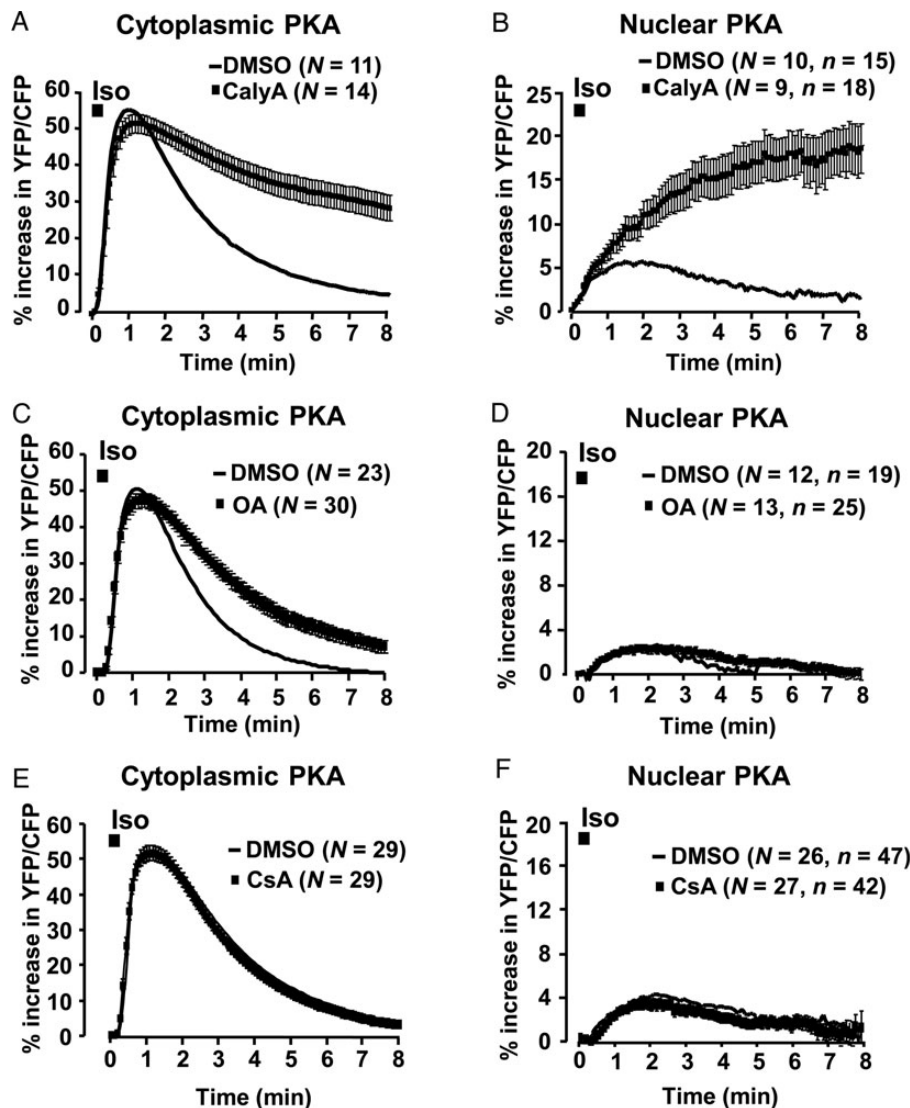


**Figure 6** Contribution of Ser/Thr PPs to the apparent PKA activity in the cytoplasm and the nuclei of ARVMs. (A and B) Effect of concomitant PP1 and PP2A inhibition with CalyA (100 nM) on cytoplasmic (A) and nuclear (B) PKA responses to Iso (100 nM, 15 s) in ARVMs. (C and D) Effect of PP2A inhibition with OA (100 nM) on Iso (100 nM, 15 s)-induced stimulation of PKA in the cytoplasm (C) and the nuclei (D) of ARVMs. (E and F) Effect of PP2B inhibition with CsA (5  $\mu$ M) on transient  $\beta$ -AR responses in the cytoplasm (E) and the nuclei (F) of ARVMs. Cells were infected with Ad.AKAR3-NES or Ad.AKAR3-NLS for 48 h. OA (black squares), CsA (black squares), or control DMSO (solid lines) were pre-incubated for 1 h at 37°C and then maintained throughout the experiments. CalyA (black squares) or control DMSO (solid lines) was applied 2 min before the 15 s pulse of Iso and then maintained throughout the experiments. Data are from 12 rats. Each symbol in A–F represents the mean  $\pm$  SEM.

*Pde4d*<sup>-/-</sup> mice.<sup>35</sup> In HEK293 cells, PDE4 inhibition dramatically accelerated the nuclear PKA response to a maintained application of forskolin, implying that PDE4 inhibition uncovered a nuclear pool of PKA in these cells.<sup>13</sup> Although the pulse stimulation used here did not allow unambiguous determination of the onset kinetics, our data do not support a similar acceleration of nuclear PKA activation by PDE4 inhibition in ARVMs (Figure 5). Rather, a different arrangement of components may exist in cardiac myocytes, with PDE4 being located at the nuclear envelope,<sup>16,25</sup> where it controls the extent of C subunits released upon  $\beta$ -AR stimulation and transferred into the nucleus from an extra-nuclear pool of PKA holoenzyme.

Our study shows that Ser/Thr PPs PP1 and PP2A contribute differently to AKAR3 dephosphorylation between the cytoplasm and the nucleus. The balanced contribution of PP1 and PP2A in the

cytoplasm is consistent with these two PPs playing a major role in controlling the phosphorylation status of ECC proteins and in counteracting the  $\beta$ -AR/cAMP/PKA-mediated functional effects in cardiac myocytes.<sup>5</sup> In contrast, PP2B inhibition had no effect, suggesting a minor participation of calcineurin in AKAR3 dephosphorylation in the bulk cytoplasm and the nuclei when PP1 and PP2A are active. A more important participation of PP2B might occur in pathological contexts, such as cardiac pressure-overload hypertrophy, where PP2B is activated.<sup>38</sup> In agreement with this hypothesis, it was reported that PP2B blunts  $\beta$ -AR phosphorylation of PLB in spontaneously hypertensive rats.<sup>39</sup> Moreover, whereas PP2B is not detected in the nuclei of normal heart, it is clearly localized in this compartment in the diseased myocardium.<sup>40</sup>

While our work was in revision, Yang et al.<sup>41</sup> published an independent report in neonatal cardiomyocytes where they found similar kinetics

differences in cytoplasmic and nuclear PKA activation, which supports activation of the PKA holoenzyme in the cytoplasm and translocation of the C subunits to the nucleus in neonatal myocytes. Yang *et al.*, however, did not investigate the role of PDE families in  $\beta$ -AR response as done here. Their modelling approach predicts a determinant role of PP activity on the amplitude of nuclear PKA response, which is consistent with what we found here.

PP1 has been shown to have crucial functions in the nucleus of other cell types.<sup>42</sup> Our data suggest that a nuclear PP1 efficiently suppresses PKA activation in the nucleus, and this could provide new opportunities to selectively manipulate nuclear  $\beta$ -AR signalling independently of ECC regulation. As stated above, it has been proposed recently that PKA favours nuclear accumulation of HDAC5, thereby inhibiting cardiomyocyte hypertrophy.<sup>9,11</sup> Thus, nuclear PP1 inhibition may enhance this cardioprotective effect of  $\beta$ -AR stimulation without increasing the phosphorylation of PLB and RyR2 as observed upon global PP1 inhibition, which—although beneficial on the short term—is associated with an increased risk of ventricular arrhythmia and the development of a progressive cardiomyopathy with aging.<sup>43</sup>

In summary, our results demonstrate for the first time that  $\beta$ -AR-stimulated PKA activity is differentially regulated in the cytoplasm and the nuclei of adult rat ventricular myocytes, and delineate the respective role of PDE3 and PDE4 and of PPs in this process. Our results unveil PP1 as a critical negative regulator of nuclear PKA in response to  $\beta$ -AR stimulation, and this should have important functional consequences for the control of nuclear PKA targets such as the CREB family of transcription factors and Class II HDACs, which are involved in pathological cardiac remodelling and in the adverse effects of chronic  $\beta$ -AR stimulation.

## Supplementary material

Supplementary material is available at *Cardiovascular Research* online.

## Acknowledgements

We thank Pierre Bobin, Dr Jérôme Leroy, and Dr Martine Pomérance for helpful discussion of the data. We also thank Valérie Nicolas (imaging core facility, University Paris-Sud, IFR 141) for assistance with confocal microscopy. We are also grateful to Dr Hazel Lum (University of Illinois) for providing the adenovirus encoding PKI and to Dr Yang K. Xiang (University of California Davis) for providing the adenovirus encoding ICUE3.

**Conflict of interest:** none declared.

## Funding

Z.H.S. was a recipient of doctoral grants from the CORDDIM program of Région Ile-de-France and from the Fondation pour la Recherche Médicale. This work was supported by ANR grant 2010 (BLAN 1139-01 to G.V.), the Fondation Leducq for the Transatlantic Network of Excellence cycAMP grant (06CVD02 to R.F.), DFG SFB (1002 TP A02 to A.E.A.) and NIH grant (R21HL107960 to W.V.R.).

## References

- Tasken K, Aandahl EM. Localized effects of cAMP mediated by distinct routes of protein kinase A. *Physiol Rev* 2004;**84**:137–167.
- Bers DM. Cardiac excitation-contraction coupling. *Nature* 2002;**415**:198–205.
- Scott JD, Santana LF. A-kinase anchoring proteins: getting to the heart of the matter. *Circulation* 2010;**121**:1264–1271.
- Mika D, Leroy J, Vandecasteele G, Fischmeister R. PDEs create local domains of cAMP signaling. *J Mol Cell Cardiol* 2012;**52**:323–329.
- Herzig S, Neumann J. Effects of serine/threonine protein phosphatases on ion channels in excitable membranes. *Physiol Rev* 2000;**80**:173–210.
- Leroy J, Abi-Gerges A, Nikolaev VO, Richter W, Lechene P, Mazet JL *et al.* Spatio-temporal dynamics of beta-adrenergic cAMP signals and L-type Ca<sup>2+</sup> channel regulation in adult rat ventricular myocytes: role of phosphodiesterases. *Circ Res* 2008;**102**:1091–1100.
- Saucerman JJ, Zhang J, Martin JC, Peng LX, Stenbit AE, Tsien RY *et al.* Systems analysis of PKA-mediated phosphorylation gradients in live cardiac myocytes. *Proc Natl Acad Sci USA* 2006;**103**:12923–12928.
- Muller FU, Neumann J, Schmitz W. Transcriptional regulation by cAMP in the heart. *Mol Cell Biochem* 2000;**212**:11–17.
- Ha CH, Kim JY, Zhao J, Wang W, Jhun BS, Wong C *et al.* PKA phosphorylates histone deacetylase 5 and prevents its nuclear export, leading to the inhibition of gene transcription and cardiomyocyte hypertrophy. *Proc Natl Acad Sci USA* 2010;**107**:15467–15472.
- Backs J, Worst BC, Lehmann LH, Patrick DM, Jebessa Z, Kreuzer MM *et al.* Selective repression of MEF2 activity by PKA-dependent proteolysis of HDAC4. *J Cell Biol* 2011;**195**:403–415.
- Chang CW, Lee L, Yu D, Dao K, Bossuyt J, Bers DM. Acute beta-adrenergic activation triggers nuclear import of histone deacetylase 5 and delays Gq-induced transcriptional activation. *J Biol Chem* 2013;**288**:192–204.
- Harootyan AT, Adams SR, Wen W, Meinkoth JL, Taylor SS, Tsien RY. Movement of the free catalytic subunit of cAMP-dependent protein kinase into and out of the nucleus can be explained by diffusion. *Mol Biol Cell* 1993;**4**:993–1002.
- Sample V, Dipilato LM, Yang JH, Ni Q, Saucerman JJ, Zhang J. Regulation of nuclear PKA revealed by spatiotemporal manipulation of cyclic AMP. *Nat Chem Biol* 2012;**8**:375–382.
- Yang J, Drazba JA, Ferguson DG, Bond M. A-kinase anchoring protein 100 (AKAP100) is localized in multiple subcellular compartments in the adult rat heart. *J Cell Biol* 1998;**142**:511–522.
- Kapiloff MS, Jackson N, Airhart N. mAKAP and the ryanodine receptor are part of a multi-component signaling complex on the cardiomyocyte nuclear envelope. *J Cell Sci* 2001;**114**:3167–3176.
- Dodge KL, Khouangsathiene S, Kapiloff MS, Mouton R, Hill EV, Houslay MD *et al.* mAKAP assembles a protein kinase A/PDE4 phosphodiesterase cAMP signaling module. *EMBO J* 2001;**20**:1921–1930.
- Dodge-Kafka KL, Soughayer J, Pare GC, Carlisle Michel JJ, Langeberg LK, Kapiloff MS *et al.* The protein kinase A anchoring protein mAKAP coordinates two integrated cAMP effector pathways. *Nature* 2005;**437**:574–578.
- Haberland M, Montgomery RL, Olson EN. The many roles of histone deacetylases in development and physiology: implications for disease and therapy. *Nat Rev Genet* 2009;**10**:32–42.
- Tomita H, Nazmy M, Kajimoto K, Yehia G, Molina CA, Sadoshima J. Inducible cAMP early repressor (ICER) is a negative-feedback regulator of cardiac hypertrophy and an important mediator of cardiac myocyte apoptosis in response to beta-adrenergic receptor stimulation. *Circ Res* 2003;**93**:12–22.
- Lewin G, Matus M, Basu A, Frebel K, Rohsbach SP, Safronenko A *et al.* Critical role of transcription factor cyclic AMP response element modulator in beta1-adrenoceptor-mediated cardiac dysfunction. *Circulation* 2009;**119**:79–88.
- DiPilato LM, Zhang J. The role of membrane microdomains in shaping beta2-adrenergic receptor-mediated cAMP dynamics. *Mol Biosyst* 2009;**5**:832–837.
- Allen MD, Zhang J. Subcellular dynamics of protein kinase A activity visualized by FRET-based reporters. *Biochem Biophys Res Commun* 2006;**348**:716–721.
- Rochais F, Vandecasteele G, Lefebvre F, Lugnier C, Lum H, Mazet JL *et al.* Negative feedback exerted by cAMP-dependent protein kinase and cAMP phosphodiesterase on subsarcolemmal cAMP signals in intact cardiac myocytes: an *in vivo* study using adenovirus-mediated expression of CNG channels. *J Biol Chem* 2004;**279**:52095–52105.
- Lum H, Jaffe HA, Schulz IT, Masood A, Raychaudhury A, Green RD. Expression of PKA inhibitor (PKI) gene abolishes cAMP-mediated protection to endothelial barrier dysfunction. *Am J Physiol* 1999;**277**:C580–C588.
- Lugnier C, Keravis T, Le Bec A, Pauvert O, Proteau S, Rousseau E. Characterization of cyclic nucleotide phosphodiesterase isoforms associated to isolated cardiac nuclei. *Biochim Biophys Acta* 1999;**1472**:431–446.
- Jin SL, Latour AM, Conti M. Generation of PDE4 knockout mice by gene targeting. *Methods Mol Biol* 2005;**307**:191–210.
- Bialojan C, Takai A. Inhibitory effect of a marine-sponge toxin, okadaic acid, on protein phosphatases. Specificity and kinetics. *Biochem J* 1988;**256**:283–290.
- Gervasi N, Hepp R, Tricoire L, Zhang J, Lambolez B, Paupardin-Tritsch D *et al.* Dynamics of protein kinase A signaling at the membrane, in the cytosol, and in the nucleus of neurons in mouse brain slices. *J Neurosci* 2007;**27**:2744–2750.
- Pereira L, Ruiz-Hurtado G, Morel E, Laurent AC, Metrich M, Dominguez-Rodriguez A *et al.* Epac enhances excitation-transcription coupling in cardiac myocytes. *J Mol Cell Cardiol* 2012;**52**:283–291.
- Metrich M, Lucas A, Gastineau M, Samuel JL, Heymes C, Morel E *et al.* Epac mediates beta-adrenergic receptor-induced cardiomyocyte hypertrophy. *Circ Res* 2008;**102**:959–965.
- McKinsey TA, Zhang CL, Olson EN. Activation of the myocyte enhancer factor-2 transcription factor by calcium/calmodulin-dependent protein kinase-stimulated binding of 14-3-3 to histone deacetylase 5. *Proc Natl Acad Sci USA* 2000;**97**:14400–14405.

32. Vega RB, Harrison BC, Meadows E, Roberts CR, Papst PJ, Olson EN et al. Protein kinases C and D mediate agonist-dependent cardiac hypertrophy through nuclear export of histone deacetylase 5. *Mol Cell Biol* 2004;**24**:8374–8385.
33. Wu X, Zhang T, Bossuyt J, Li X, McKinsey TA, Dedman JR et al. Local InsP3-dependent perinuclear  $Ca^{2+}$  signaling in cardiac myocyte excitation-transcription coupling. *J Clin Invest* 2006;**116**:675–682.
34. Xiang Y, Naro F, Zoudilova M, Jin SL, Conti M, Kobilka B. Phosphodiesterase 4D is required for  $\beta_2$  adrenoceptor subtype-specific signaling in cardiac myocytes. *Proc Natl Acad Sci USA* 2005;**102**:909–914.
35. Lehnart SE, Wehrens XH, Reiken S, Warrier S, Belevych AE, Harvey RD et al. Phosphodiesterase 4D deficiency in the ryanodine-receptor complex promotes heart failure and arrhythmias. *Cell* 2005;**123**:25–35.
36. Beca S, Helli PB, Simpson JA, Zhao D, Farman GP, Jones PP et al. Phosphodiesterase 4D regulates baseline sarcoplasmic reticulum  $Ca^{2+}$  release and cardiac contractility, independently of L-type  $Ca^{2+}$  current. *Circ Res* 2011;**109**:1024–1030.
37. Pare GC, Bauman AL, McHenry M, Michel JJ, Dodge-Kafka KL, Kapiloff MS. The mA<sub>K</sub>AP complex participates in the induction of cardiac myocyte hypertrophy by adrenergic receptor signaling. *J Cell Sci* 2005;**118**:5637–5646.
38. Lim HW, De Windt LJ, Steinberg L, Taigen T, Witt SA, Kimball TR et al. Calcineurin expression, activation, and function in cardiac pressure-overload hypertrophy. *Circulation* 2000;**101**:2431–2437.
39. MacDonnell SM, Kubo H, Harris DM, Chen X, Berretta R, Barbe MF et al. Calcineurin inhibition normalizes beta-adrenergic responsiveness in the spontaneously hypertensive rat. *Am J Physiol Heart Circ Physiol* 2007;**293**:H3122–H3129.
40. Hallhuber M, Burkard N, Wu R, Buch MH, Engelhardt S, Hein L et al. Inhibition of nuclear import of calcineurin prevents myocardial hypertrophy. *Circ Res* 2006;**99**:626–635.
41. Yang JH, Polanowska-Grabowska RK, Smith JS, Shields CW IV, Saucerman JJ. PKA catalytic subunit compartmentation regulates contractile and hypertrophic responses to beta-adrenergic signaling. *J Mol Cell Cardiol* 2013;**66C**:83–93.
42. Bollen M, Beullens M. Signaling by protein phosphatases in the nucleus. *Trends Cell Biol* 2002;**12**:138–145.
43. Wittkopper K, Fabritz L, Neef S, Ort KR, Grefe C, Unsold B et al. Constitutively active phosphatase inhibitor-1 improves cardiac contractility in young mice but is deleterious after catecholaminergic stress and with aging. *J Clin Invest* 2010;**120**:617–626.